Controlled blunt impact experiments on soft tissue simulants

Timothy J. Beavers[1,2], Abhijit Chandra[1], and Sarah A. Bentil[1,2]
[1] Department of Mechanical Engineering, Iowa State University;
[2] The Bentil Group, Department of Mechanical Engineering, Iowa State University

ABSTRACT

Traumatic brain injury (TBI) following blunt force impact to the head yields symptoms that include confusion, headache, dizziness, and speech problems. The injury mechanism resulting in these symptoms is still not well understood, hindering the development of effective countermeasures. To increase our understanding of TBI (without skull fracture), we have designed an apparatus that can reproduce blunt impact forces in a controllable and repeatable manner. The apparatus consists of a simplistic cylindrical head system with tissue and fluid surrogates to represent the brain, cerebrospinal fluid (CSF), and skull. Resultant forces imparted on the outer layer of the skull are recorded using force transducers. A tri-axial accelerometer mounted on the brain and a laser vibrometer are used to measure the acceleration and velocity, respectively. A dedicated shaker is coupled with the head system (i.e. brain-CSF-skull apparatus) to allow for controlled and repeatable testing of blunt loading scenarios of variable complexities. The selection of the shaker's frequency and applied force needed to simulate a TBI, such as a concussion, were guided by the Severity Index (SI) scale. The SI scale is used to rate the severity of skull impact. SI of 700 corresponds to a concussion sustained by a National Football League (NFL) player during gameplay. The duration of the blunt impact resulting in concussion is 15 ms, which translates to an acceleration of 74 g-force. Our preliminary results show that when the shaker's period of oscillation was 15 ms, a maximum acceleration of 49 g-force and a measured resultant skull force of 196.6 N was recorded. At 15 ms, the percent difference for the acceleration measured using our head system and 74 g-force reported by the SI scale is 41%. To ensure that a TBI event is being reproduced using the brain-CSF-skull apparatus, the mass on the unbalanced shaker tray will be increased until the acceleration matches 74 g-force. Our brain-CSF-skull apparatus will facilitate research to identify the various frequencies and loading magnitudes that will yield a TBI. The results of the research will aid in the design of countermeasures to damping or offset the frequencies experienced by the brain resulting in TBI.

INTRODUCTION

According to the Centers for Disease Control (CDC), approximately 2.8 million traumatic brain injury (TBI) related Emergency Department (ED) visits occurred annually between 2007 and 2013. From those TBI-related ED visits, 56,000 patients a year died (Taylor, 2017). In 2013, the World Health Organization (WHO) reported that the annual death worldwide attributed to TBI was 1.3 million (World Health Organization, 2013). Thus, TBI is a public health issue that remains unresolved and requires continued attention by researchers.

TBI research includes the design and fabrication of protective devices (e.g. helmets) for the human head, and also experiments and computational modeling of blast and blunt impact events to understand injury mechanisms. Research in helmet design has resulted in a reduction of skull fracture following blunt impact. However, TBI still occurs due to the lack of research exploring the correlation between the helmet and head as a dynamic system.

Advances in computer computational capacity have attracted researchers to simulate blunt impact events using finite element analysis (FEA), as a means to predict the motion and forces inside of a head. These computational models require significant time to simulate the response of the head following impact. So, populating a large database with resultant forces from a given blunt impact event is not practical. Furthermore, blunt impact experimental data of the head is needed to validate the computational models. Current experiments examine a specific injury mechanism or impact scenario, or is based on cadaver or animal testing (E.S. Gurdjian et al. 1970; C. Ljung, 1975; Susan Margulies, 1990). Yet, TBI still occurs due to the lack of experiments that can simultaneously analyze the dynamic response of the brain, cerebrospinal fluid (CSF), and skull system. Understanding the connection between the motion of the brain and TBI, using the brain's frequency response following blunt impact, will aid in the design of countermeasures. These countermeasures should isolate and mitigate the frequencies that will lead to the long term neurologic and functional effects of individuals (e.g. professional athletes) experiencing Repeated Head Impacts (RHI).

The primary intent of this research is to design and validate a modular apparatus for testing a brain-CSF-skull under varying blunt impact events. The apparatus measures the resultant skull force, while exciting a brain surrogate. Measurements of the brain's acceleration at various blunt event durations were used to calculate its resultant forces. Once the design is validated, the system can then be modified by considering other materials and geometries to describe the brain and skull surrogate.

METHODS

Specimen Setup

To calibrate and ensure that the measured acceleration and forces of the brain-CSF-skull apparatus was repeatable, homogeneous materials were selected for the brain and skull surrogate, and water served as the CSF. After calibrating the apparatus, the materials and geometry for the brain and skull be modified to explore the effect of varying material properties and geometries on the measured acceleration and force. Actual tests utilized lower durometer and non-homogenous materials to simulate the brain, as well as varying skull surrogates (e.g. nylon).

For simplicity in simulating blunt impact to the head, a cylindrical geometry was selected for the brain and skull (Figure 1). The brain cylinder's diameter and length were 101.6 mm and 203.2 mm, respectively. These dimensions were selected by considering the dimensions of a human brain, which is more oblong than spherical. An average adult brain has a length of 165 mm, width of 140 mm, and height of 91 mm.

The cylinder's length was twice the diameter. The relationship between the cylinder's length and diameter allowed the three-dimensional problem to be reduced to two-dimensions (x-y plane) by classifying the geometry as "infinitely long".

Two different cylindrical rubber samples were sandwiched together, using DOW Great Stuff™ Pond & Stone insulating foam, to create an inhomogeneous brain surrogate. An aluminum cylinder passes through the center of the brain-CSF-skull assembly to connect to the shaker system. This connection simulates blunt impact by causing the brain surrogate to impact the skull surrogate.

The gap between the skull surrogate and outer brain cylinder is filled with a CSF simulant. Buna-N sheets (shown in red in Figure 1) are clamped to the skull to seal the brain and CSF. The base and top of the apparatus have bulkhead connectors to fill the CSF layer and facilitate draining of the fluid following experiments. To simulate different CSF pressures ranging from normal (0-10 mmHg gauge) and abnormal (20-25 mmHg gauge), the pressure inside the system can be adjusted using these bulkhead connectors (Ghajar, 2000).

Future iterations of the brain-CSF-skull system will increase in complexity by considering a head system with geometries ranging from spherical to oblong shape. Finally, an additive manufacturing procedure will be considered in the future to create complex and biofidelic human skull geometries; as well as utilizing epoxy materials to fabricate brain surrogates with material properties that are characteristic of live tissue.

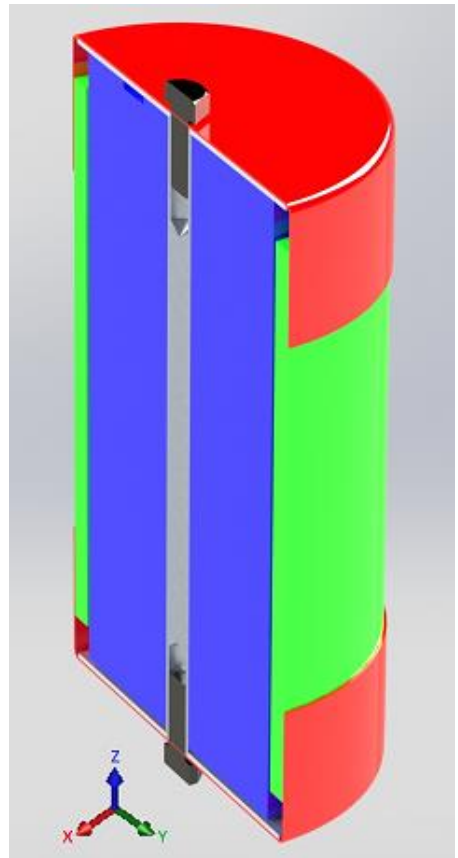

Figure 1: Cut-away of brain-CSF-skull configuration. Two center brain cylinders (blue) of different durometer materials (75A and 40A). Outer cylinder (green) represents the skull (green). Sealing the system at top and bottom is a 40A durometer Buna-N sheet. Aluminum rod (gray) passes through center of brain. CSF layer is between the brain (blue) and skull (green).

Test Apparatus

The primary purpose of this research is the creation of a modular apparatus that can simulate realistic blunt impact impulses to the head and is instrumented with force and acceleration sensors. After the shaker system excites the brain, the brain-CSF-skull system's frequency response is analyzed using the resultant forces measured by the force transducers attached to the

skull surrogate. A tri-axial accelerometer and laser vibrometer was used to measure the acceleration and velocity of the brain assembly, respectively.

To add redundancy as well as increase accuracy of the measured forces, the force transducers were arranged in a triangular orientation (Figure 2). The force in the desired axis of excitation is measured by the first force transducer labeled as F_1 (Figure 3). The opposing two force transducers (F_2 and F_3) are offset by 30° from either side of the desired axis of excitation. This force transducer arrangement allowed for the calculation of the off-kilter impact events. Accuracy of the calculated incident force value is increased due to the triangular arrangement, by removing the restriction that the axis of excitation from the shaker should align with F_1. Trigonometry can be applied to calculate the exact axis of excitation, along with the maximum impact amplitude (magnitude of F_i). The tri-axial accelerometer coupled with the force transducers provides the peak acceleration in the axis of excitation of the brain.

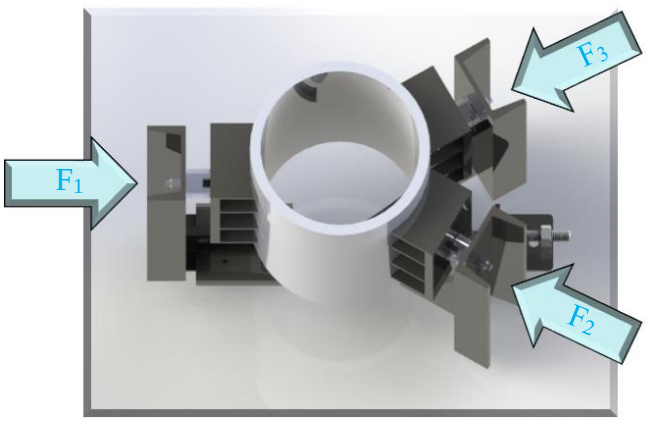

Figure 2: Arrangement of force transducers (counter-clockwise from left: F_1, F_2, and F_3) around the perimeter of the skull used to measure the skull resultant forces needed to calculate the incident force (F_i) and angle (ϕ). Shown is a three-dimensional view of a skull cylinder between the force transducer array. The brain and CSF layer is not shown for clarity.

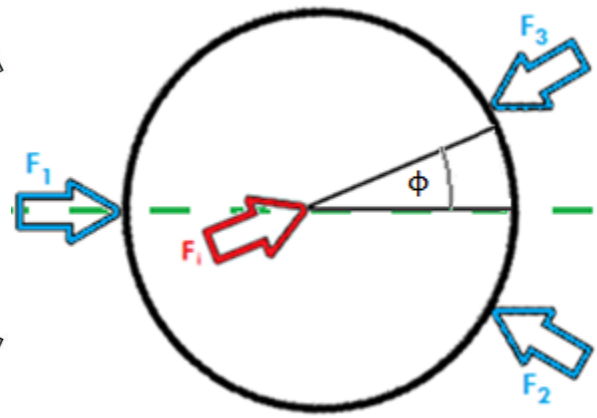

Figure 3: Arrangement of force transducers (F_1, F_2, and F_3) around the perimeter of the skull to allow for determination of the incident force (F_i) and angle (ϕ). Axis of excitation is shown as green dashed line.

To affix the rod passing through the center of the brain-CSF-skull system to the shaker assembly, a C-frame support was constructed using 6061 aluminum (Figure 4). The C-frame was designed to be light weight to maximize the acceleration applied to the brain surrogate and a t-channel shape was chosen to maximize the C-frame's strength in the y-axis. The C-frame assembly is suspended by two chains to fix the motion in the z-axis, but free motion in the x-y plane. The shaker assembly is connected to the opposite side of the C-frame, to allow transmission of the desired blunt impacts to the brain-CSF-skull apparatus. The accelerometer is attached to the top of the C-frame and is placed within 20 mm of the rod passing through the center of the brain. In this way, deflection of the C-frame does not influence the acceleration measurement. Reaching a minimum excited mass of 6.05 kg allows for maximizing the brain sample's acceleration. Since

the accelerometer measurement is located near the desired measurement point of the brain center, structural deflection of the C-frame does not influence this measurement.

For the skull, a separate rigid assembly was designed to minimize the deflection following impact of the brain surrogate due to excitation of the C-frame assembly. Sandwiched between the skull support frame and the skull were the three force transducers. Pre-loading the force transducers was needed to support the skull cylinder; approximately 89 N (for F_1) and 103 N (for F_2 and F_3). Mild steel was used to form the base frame and skull supports, which contoured the skull and equally distributed the incident forces from the skull to each respective force transducer.

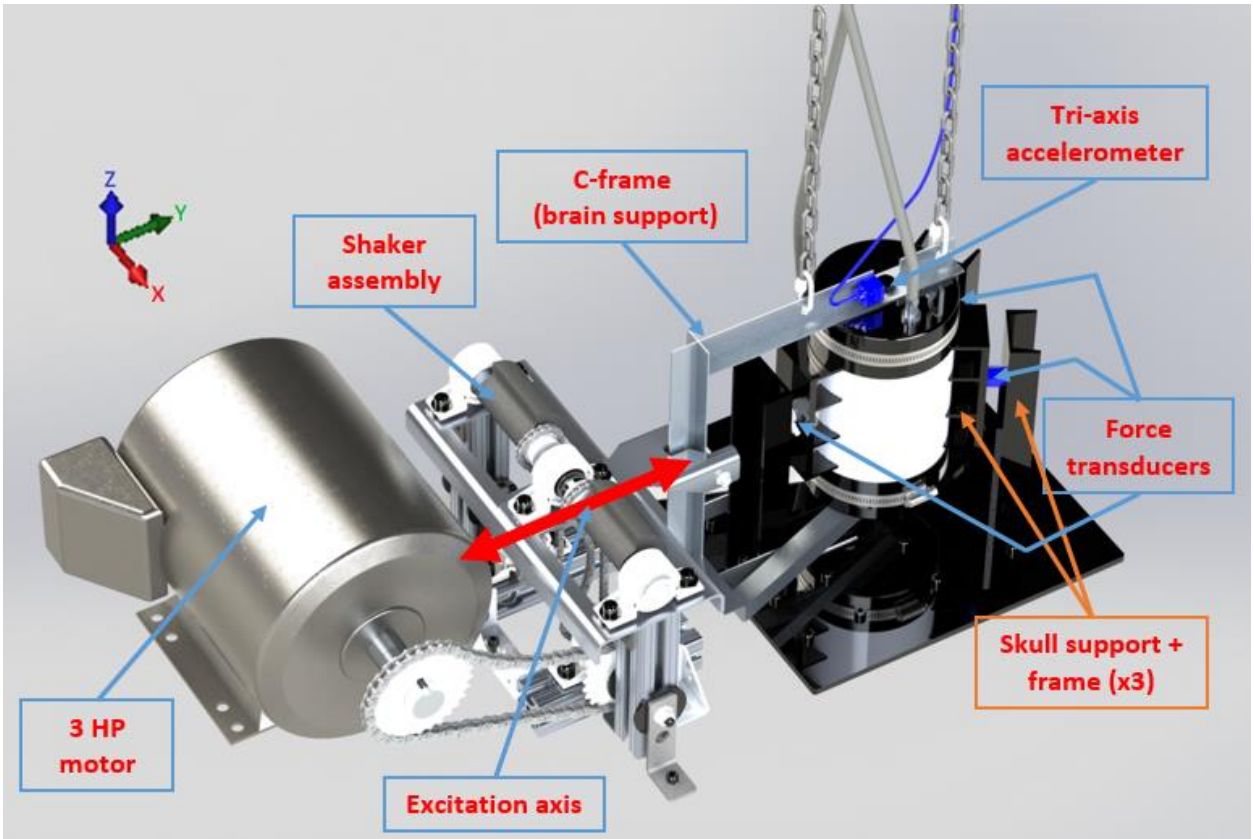

Figure 4: Complete brain-CSF-Skull apparatus includes a shaker assembly driven by 3 HP electric motor. Shaker assembly imparts cyclical impulses along excitation axis.

Ideally an electronic shaker would apply varying amplitudes and frequency impulses to the C-frame. However, due to the cost, size envelope, and excessive capabilities of commercially available electronic shakers, a mechanical shaker was selected for the brain-CSF-skull apparatus. To maximize the incident force while still allowing for variability in event duration, an unbalanced rotating assembly was utilized for the shaker function. By varying the counterbalance mass (Figure 6) and rotation speed of the shaker assembly, different impact durations, forces, and accelerations could be applied to the brain-CSF-skull system.

Testing conditions

To increase understanding of blunt impact conditions leading to TBI, a database consisting of the resultant skull force from varying event accelerations, durations, and scenarios (e.g. different

CSF pressures, brain-CSF-skull geometries, and material properties) is proposed. This resultant skull force is calculated using force transducer measurements. Coupling the resultant skull force with the experimental results from the brain-CSF-skull apparatus will facilitate interpolation of brain-CSF-skull parameters and event conditions to predict the onset and/or severity of TBI, without the need for additional tests. Furthermore, the proposed dataset will be invaluable in FEA by providing variables, such as expected forces, displacements, and velocities, that can be used for validation. To calibrate the brain-CSF-skull system design, before increasing geometric and material complexity, the initial database consists of a series of baseline tests as described in the Specimen Setup section.

The primary measurement being analyzed is the resultant skull force. For a given event acceleration and duration with a known mass, an expected resultant force can be derived similar to the Head Injury Criterion (HIC). HIC is a useful criterion for determining injury severity following a blunt impact event, given information about time (t) and acceleration (a), as shown in equation 1. Varying the shaker results in different impact durations, while changes in the acceleration is obtained through the addition/subtraction of counterbalance weights. The peak force, event duration, and peak acceleration obtained with the brain-CSF-skull apparatus can be compared with blunt impact events to the head and HIC. Currently, HIC does not include information about the forces and resonant frequencies associated with the blunt impact.

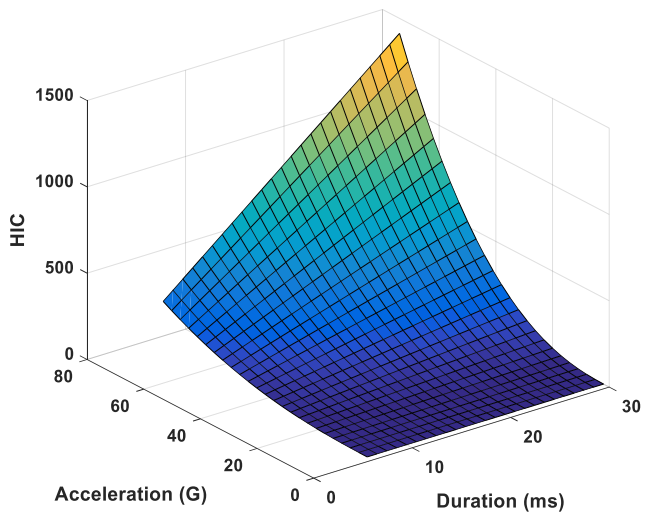

Figure 5: Three-dimensional surface plot of HIC. Event durations range between 6 ms to 30 ms and accelerations between 2 and 74 g-force.

$$HIC = \left(\frac{1}{t_2 - t_1}\int_{t_1}^{t_2} a(t)dt\right)^{2.5}(t_2 - t_1) \qquad \text{(Eq. 1)}$$

During testing of the brain-CSF-skull system, the shaker frequency is infinitely variable due to the variable frequency drive motor However, six discrete steps were used as they are easily divisible by the motor frequency of 0 to 60 Hz. The slowest frequency impact event requires 90 ms to complete, while the fastest frequency event required a total of 15 ms.

The unbalanced masses of the shaker assembly varied between two settings: 1.23 kg and 0.61 kg. Based on the unbalance mass (m) and its centroid (r), the unbalance (U) is calculated (equation 2). Clarification of the unbalance mass, unbalance centroid, and counterweight shape is depicted in Figure 6.

$$U = m\,x\,r \qquad \text{(Eq. 2)}$$

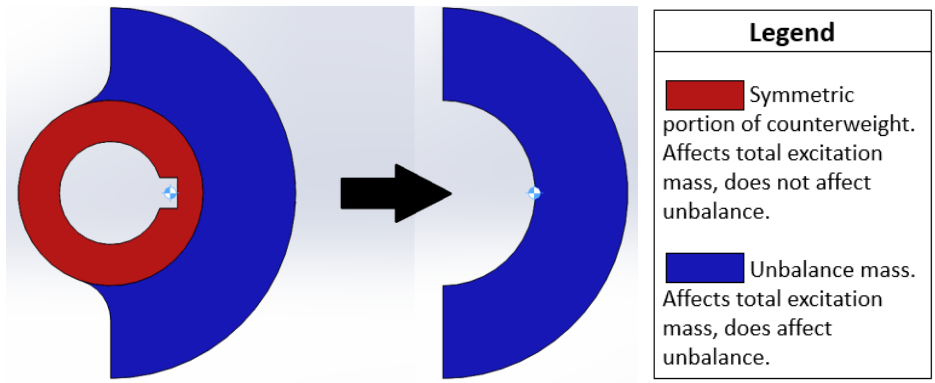

Figure 6: Unbalance mass and centroid shown in relation to total counterweight mass and centroid. Equation 2 and 3 apply the unbalance mass and unbalance centroid.

Two U settings (U = 0.01675 kg*m and U = 0.00838 kg*m) were calculated using the previously mentioned mass settings. By varying the unbalance mass and rotational speed (ω), different incident forces are obtained. Using equation 3, the resultant force (F) created from the shaker can be calculated using unbalance and rotational speed. When the excited mass is constant, the acceleration can be calculated using the force equation (equation 4), and this result can be validated with the accelerometer measurements.

$$F = U\ x\ \omega^2 \qquad \text{(Eq. 3)}$$

$$F = m\ x\ a \qquad \text{(Eq. 4)}$$

Each combination of U should follow a curved line along the event duration and acceleration axes on a graph similar to HIC (Figure 5), with the dependent axis being resultant skull force instead of HIC.

Data analysis

The force transducer arrangements facilitated adjustment of the brain-CSF-skull apparatus to minimize off impact-axis events. Also, the unbalance shaker system was able to consistently cause the brain surrogate to impact the skull. Varying the shaker speed resulted in fluctuating impact angles. However, the varying impact angles were not an issue since the resultant impact force could be calculated from the force transducer arrangement without physically adjusting the shaker apparatus each time the speed is changed. Equations 5 and 6 are used to calculate the incident impact angle and incident impact force, respectively, which is necessary to conduct the experiments in a quick and repeatable manner without altering the apparatus.

$$\phi = \tan^{-1}\left(\frac{F_3 \sin 30° - F_2 \sin 30°}{-F_1 + F_3 \cos 30° + F_2 \cos 30°}\right) \qquad \text{(Eq. 5)}$$

$$F_i = \frac{F_3 \sin 30° - F_2 \sin 30°}{\sin \phi} \qquad \text{(Eq. 6)}$$

Before each sample run, the shaker was stationary and the measured force and accelerometer reading output was zero (or non-energized state). Following each sample run, the accelerometer and force transducer data was filtered using a low pass filter (fourth-order Butterworth with a 3 kHz cut-off frequency). The accelerometer data was integrated to calculate the velocity, which was used to validate the filter specifications. The velocity range, during validation testing of the accelerometer, was repeatable when the impact events achieved steady state. Otherwise, the velocity was affected by inertia due to the acceleration/deceleration of the shaker assembly. Just as the accelerometer data could be compared to force data from the shaker force calculations in equations 3 and 4, integrated velocity data can be compared with velocity measurements from the vibrometer.

RESULTS

The results presented in this section pertain to the calibration of the brain-CSF-skull system. Initial baseline testing of the accelerometer using a 500 Hz sample rate did not produce meaningful results. The sample rate was increased until the hardware in use presented the next bottleneck. This next limitation resulted in a maximum data acquisition sample rate of 3.2 kHz.

Figure 7 illustrates the presence of noisy data when the cut-off frequencies are below 2000 Hz. Above 2000 Hz, the velocities start to converge to the unfiltered data since the low pass filter is no longer effective.

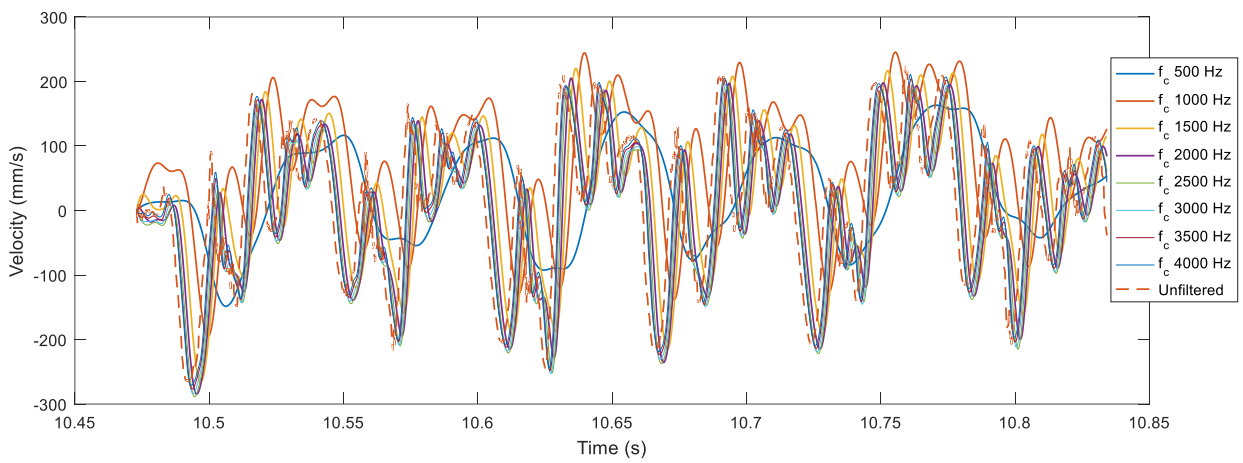

Figure 7: Brain surrogate velocities for 15.2 ms duration with varying cut-off frequencies analyzed from 500 – 4000 Hz compared to unfiltered velocities.

To show the effects of over filtering the lower frequencies from the integrated accelerometer data, the cut-off frequencies above 2000 Hz have been omitted from Figure 8.

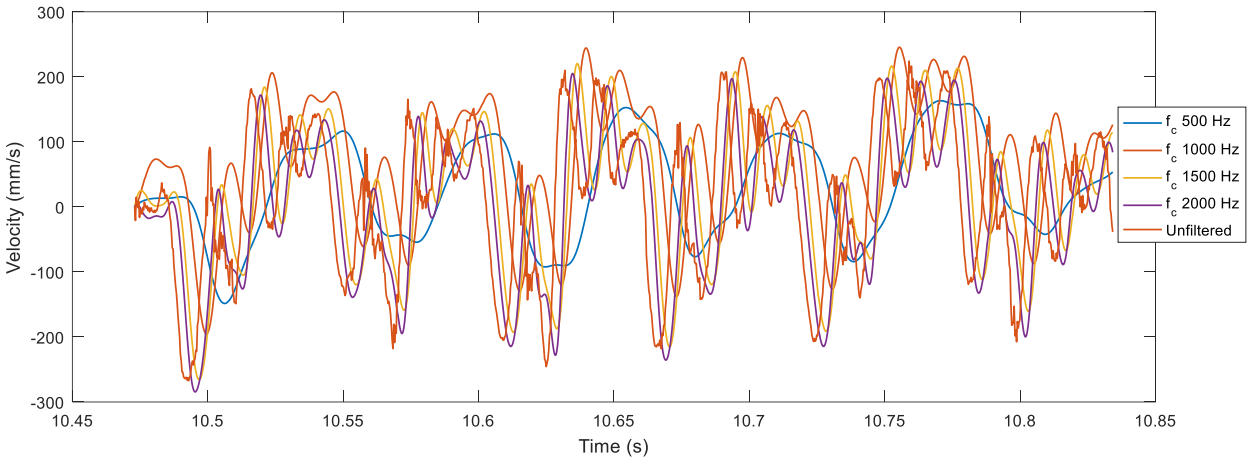

Figure 8: Brain surrogate velocities for 15.2 ms duration with 500 – 2000 Hz cut-off frequencies compared to the unfiltered velocities.

The integrated acceleration data helped reveal the effect of varying the cut-off frequency and produced velocity curves comparable with the unfiltered data. Selection of an acceptable cut-off frequency was obtained by taking the double integral of acceleration to obtain the displacement of the surrogate brain shown in Figure 9.

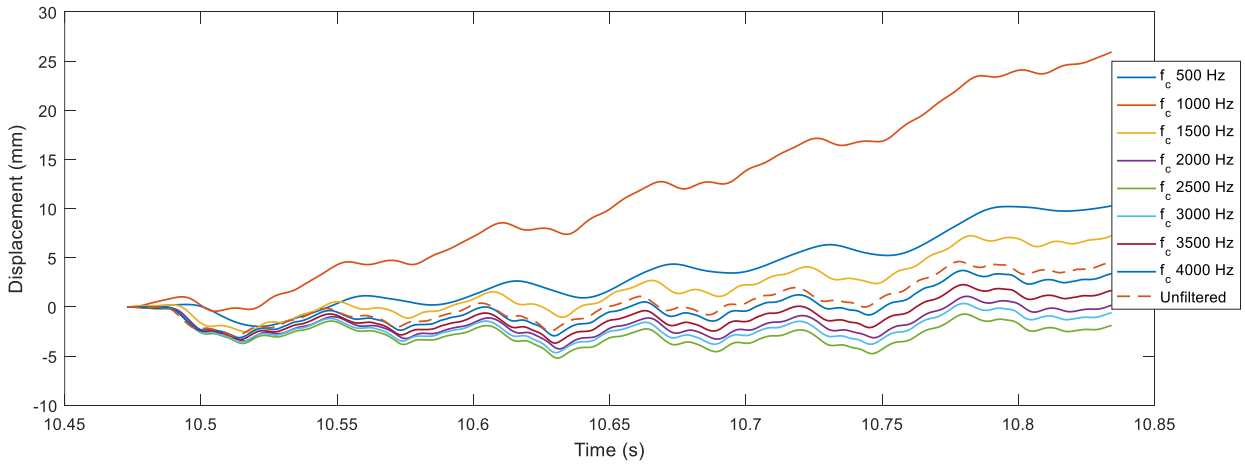

Figure 9: Brain surrogate displacements for 15.2 ms duration with varying cut-off frequencies.

Since cut-off frequencies below 2000 Hz impacted the filtered velocity, the displacements derived from the velocities were also unrealistic. Figure 9 shows that below 2000 Hz, the displacement of the brain surrogate with respect to time continued to increase. The cut-off frequencies oscillate between over-filtering and under-filtering when analyzed as displacements. In Figure 9, over- and under-filtering can be seen with the displacements at the right side of the graph. 1500 Hz and 500 Hz are under-filtered and lie above the unfiltered line while 3500 Hz and 2500Hz are over-filtered and below the unfiltered line. The two cut-off frequencies which are most realistic in terms of expected displacement: 2000 Hz, 2500 Hz, and 3000 Hz.

The accelerometer is located at the site of impact, so additional calculations from multiple sensors to determine a resultant value is not needed. Figure 10 shows the accompanying derived incident forces at varying cut-off frequencies between 1000 Hz and 4000 Hz, as well as the raw unfiltered calculation. This steady-state data set encompasses six impact events.

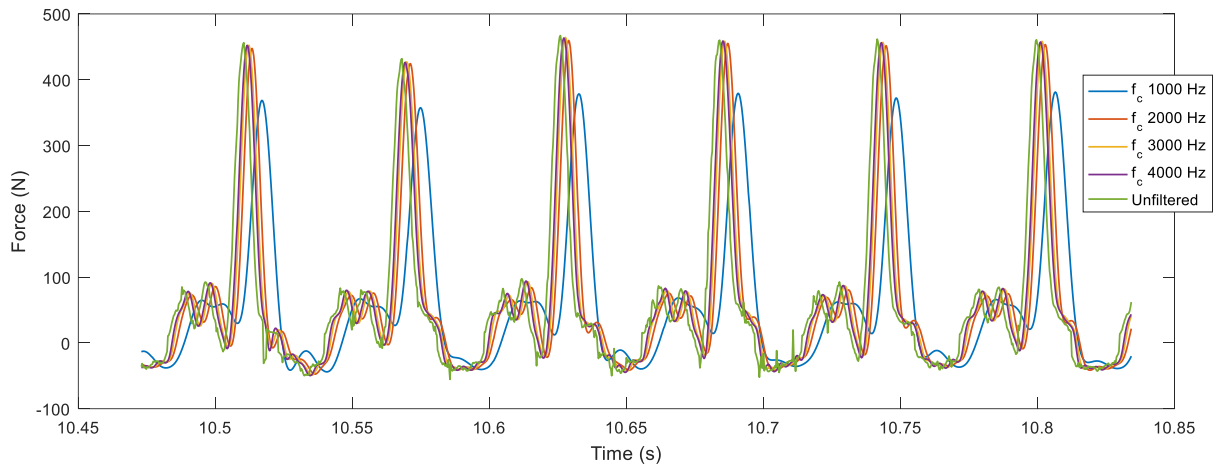

Figure 10: Skull surrogate incident forces for 15.2 ms duration with varying cut-off frequencies. Each peak corresponds to an impact event. For the given duration, 6 impact events are shown.

Force and acceleration data was collected for four different event durations (15.2 ms, 35.5 ms, 47.8 ms, and 69.5 ms). The four event durations corresponded to four different motor speeds: 660, 990, 1320 and 1650 rpm. These correlate to variable-frequency drives (VFD) of 20, 30, 40, and 50 Hz. Table 1 shows the impact events in greater detail as well as duration and force errors. The incident force increases exponentially as the event duration decreases, so the resultant error as a percentage also decreases exponentially. With the exponential increase in resultant force and HIC, the ability for the brain-CSF-skull apparatus to simulate blunt impact that can result in severe TBI level, is likely.

Table 1: Test data from validation runs

Event duration			**Forces measured**	
Event duration (ms)	**Number of impact events**	**Duration error (ms)**	**Average force (N)**	**Force error (N)**
15.22	6	$\frac{+0.78}{-0.82}$	449.4	$\frac{+9.65}{-17.43}$
35.46	12	$\frac{+6.64}{-5.06}$	165.6	$\frac{+11.70}{-16.66}$
47.76	12	$\frac{+5.04}{-10.46}$	71.5	$\frac{+18.44}{-6.69}$
69.52	8	$\frac{+7.68}{-8.52}$	4.95	$\frac{+0.79}{-0.91}$

A comparison of the four data points collected from the brain-CSF-skull apparatus can be made with the HIC surface plot from Figure 5 and is shown in Figure 11. Using the same acceleration and duration scale, the resultant skull forces increase in a similar manner to HIC.

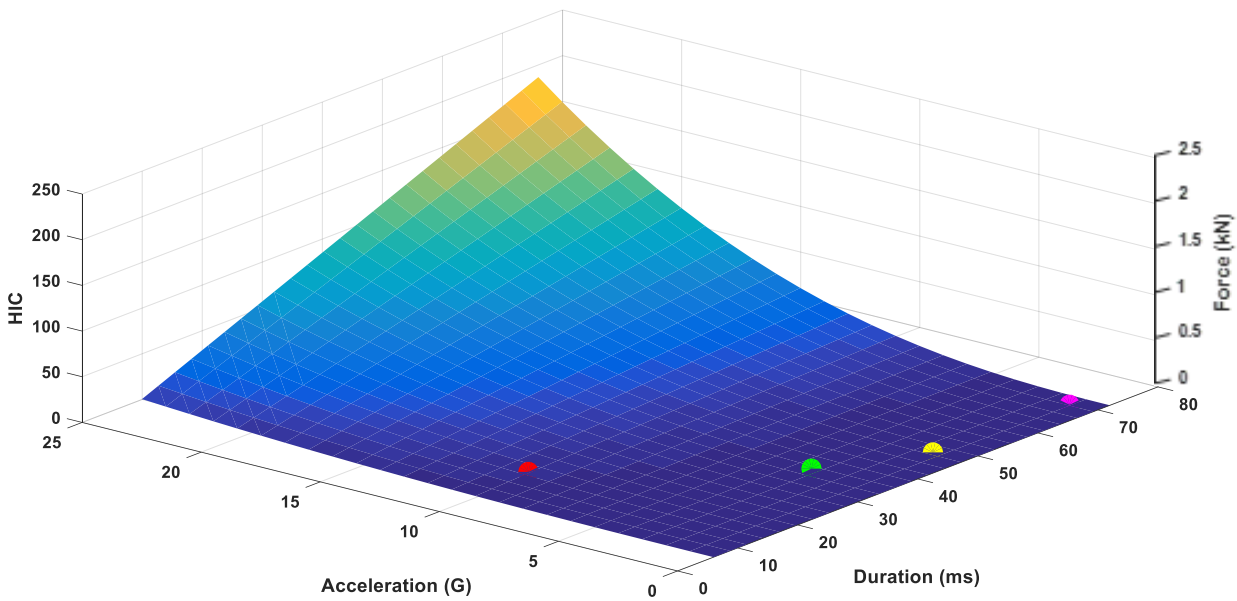

Figure 11: Brain-CSF-skull data points for four event durations (red, green, yellow and magenta points) overlaid on HIC surface plot. Surface plot has dependent variable HIC while measured data points values are forces (kN) shown on secondary z-axis.

DISCUSSION

The aim of this project is to design and validate an apparatus to simulate blunt impact to the head that may result in TBI. The apparatus is designed to be modular and can operate in a controllable and repeatable manner. Calibration and baseline measurements using the apparatus have been performed. A design of experiments (DOE) has been identified to allow statistical analysis of factors influencing TBI: event duration, acceleration, and resultant skull force.

It was observed that testing at higher impact speeds (i.e. shorter impact durations) produced repeatable and realistic results when compared with the slower impact speeds. The inertia of the counterbalance assembly also increased repeatability, since the higher inertia helped the brain-CSF-skull system operating at steady state. Unrealistic results obtained at slower impact speeds were attributed to the presence of stiction at the various pivot points of the mechanical shaker assembly and lower inertia at lower rotational speeds. Slower impact speeds yielded data that was less repeatable and the error in the measured resultant force and accelerations was higher. The preliminary data presented show accelerations as high as 49 g-force and a resultant skull force of 196.6 N, for the brain-CSF-skull apparatus. The highest resultant force obtained was not at the full shaker speed, but at the first weight setting of the counterbalance tray (0.61 kg).

Adjustment/balancing of the shaker assembly will improve the repeatability of impact events; which after filtering, increases the accuracy of calculated resultant forces. The lower HIC values are comparable with the preliminary measurements using the brain-CSF-skull apparatus. For example, low resultant force events yield low HIC scale values. The error for these low force events are high, but is not of concern since injury is not predicted.

The brain-CSF-skull apparatus can reproduce RHI level conditions. Using the HIC formula (equation 1), a 69.52 ms event with an average peak acceleration of 1.08 g-force yields a HIC value of <0.01. Contrarily, a 15.52 ms event at 9.90 g-force has a force error of $\frac{+2.1}{-3.9}$%, and a calculated HIC value of 4.8. Lower force error due to increased event duration improve the accuracy of predicting TBI and is supported by higher HIC values. Through increasing of the resultant force applied to the brain and decreasing the event duration, we hope to better understand frequency responses of the brain-CSF-skull system.

CONCLUSIONS

A brain-CSF-skull apparatus is designed to simulate blunt impact of a surrogate brain impacting a skull. Tuning the force and acceleration measurements, along with calibration of the device have been performed. Preliminary results show that the calculated resultant force is consistent with HIC curves. The next phases involve performing tests using a full-factorial design of experiment (DOE) strategy. The modular apparatus can support complex brain and skull geometries and material to aid in understanding the brain-CSF-skull's dynamic response given varying impact accelerations and durations. Results from the brain-CSF-skull apparatus will add to the body of knowledge regarding TBI mechanisms and parameter values for countermeasure development.

ACKNOWLEDGEMENTS

This project has been financially supported by start-up funds to SA Bentil from Iowa State University. The apparatus design is based on a modified version of Dr. Abhijit Chandra's Ph.D. thesis project: The Normal Approach, Contact and Rebound of Lubricated Cylinders [1980]. Many thanks to Taylor Schweizer and Jim Dauetremont at Iowa State University in design and troubleshooting the data acquisition equipment needed to perform the measurements.

REFERENCES

Bayly, P., Cohen, T., Leister, E., Ajo, D., Leuthardt, E., & Genin, G. (2005). Deformation of the human brain induced by mild acceleration. *Journal of Neurotrauma*, *22*(8), 845–856.

Chandra A. (1980, June). *The Normal Approach, Contact, and Rebound of Lubricated Cylinders*. University of New Brunswick.

Cormier, J., Manoogian, S., Bisplinghoff, J., Rowson, S., Santago, A., McNally, C., … Bolte, J. (2011). The tolerance of the maxilla to blunt impact. *Journal of Biomechanical Engineering*, *133*(6), 064501.

Faul, M., Wald, M. M., Xu, L., & Coronado, V. G. (2010). Traumatic brain injury in the United States; emergency department visits, hospitalizations, and deaths, 2002-2006.

Gadd, C. W. (1966). *Use of a weighted-impulse criterion for estimating injury hazard* (No. 0148–7191). SAE Technical Paper.

Ghajar, J. (2000). Traumatic brain injury. *The Lancet*, *356*(9233), 923–929.

Gurdjian, E., Hodgson, V., & Thomas, L. (1970). Studies on mechanical impedance of the human skull: preliminary report. *Journal of Biomechanics*, *3*(3), 239IN1241-240247.

Gurdjian, E. S., Lissner, H. R., Evans, F. G., Patrick, L. M., & Hardy, W. G. (1961). Intracranial pressure and acceleration accompanying head impacts in human cadavers. *Surgery, gynecology & obstetrics*, *113*, 185.

Hardy, W. N., Foster, C. D., Mason, M. J., Yang, K. H., King, A. I., & Tashman, S. (2001). Investigation of Head Injury Mechanisms Using Neutral Density Technology and High-Speed Biplanar X-ray. *Stapp Car Crash Journal*, *45*, 337–368.

Hodgson, V., Gurdjian, E., & Thomas, L. (1966). Experimental skull deformation and brain displacement demonstrated by flash x-ray technique. *Journal of Neurosurgery*, *25*(5), 549–552.

Johnson, E., & Young, P. (2005). On the use of a patient-specific rapid-prototyped model to simulate the response of the human head to impact and comparison with analytical and finite element models. *Journal of Biomechanics*, *38*(1), 39–45.

Kenner, V. H., & Goldsmith, W. (1973). Impact on a simple physical model of the head. *Journal of Biomechanics*, *6*(1), 1–11.

Langlois, J. A., Rutland-Brown, W., & Wald, M. M. (2006). The epidemiology and impact of traumatic brain injury: a brief overview. *The Journal of Head Trauma Rehabilitation*, *21*(5), 375–378.

Ljung, C. (1975). A model for brain deformation due to rotation of the skull. *Journal of Biomechanics*, *8*(5), 263–274

Lubock, P., & Goldsmith, W. (1980). Experimental cavitation studies in a model head-neck system. *Journal of Biomechanics*, *13*(12), 1041–1052.

Margulies, S. S., Thibault, L. E., & Gennarelli, T. A. (1990). Physical model simulations of brain injury in the primate. *Journal of Biomechanics*, *23*(8), 823–836.

Moss, W. C., King, M. J., & Blackman, E. G. (2009). Skull flexure from blast waves: a mechanism for brain injury with implications for helmet design. *Physical Review Letters*, *103*(10), 108702.

Nahum, A. M., Smith, R., & Ward, C. C. (1977). Intracranial Pressure Dynamics During Head Impact. SAE International.

Roberts, S. B., Ward, C. C., & Nahum, A. M. (1969). Head trauma — A parametric dynamic study. *Journal of Biomechanics*, *2*(4), 397–415.

Taylor, C. A. (2017). Traumatic brain injury–related emergency department visits, hospitalizations, and deaths—United States, 2007 and 2013. *MMWR. Surveillance Summaries*, *66*.

Trosseille, X., Tarriere, C., Lavaste, F., Guillon, F., & Domont, A. (1992). *Development of a FEM of the human head according to a specific test protocol* (No. 0148–7191). SAE Technical Paper.

Versace, J. (1971). *A review of the severity index* (No. 0148–7191). SAE Technical Paper.

World Health Organization. Violence, Injury Prevention, & World Health Organization. (2013). *Global status report on road safety 2013: supporting a decade of action*. World Health Organization.